Cellular & Molecular Immunology (2018) 15, 58–73

www.nature.com/cmi

RESEARCH ARTICLE

Extracellular ADP facilitates monocyte recruitment in bacterial infection *via* ERK signaling

Xiaoyu Zhang[1], Juliang Qin[1], Junyan Zou, Zhangsheng Lv, Binghe Tan, Jueping Shi, Yihan Zhao, Hua Ren, Mingyao Liu, Min Qian and Bing Du

As the most prominent clinical drug targets for the inhibition of platelet aggregation, $P2Y_{12}$ and $P2Y_{13}$ have been found to be highly expressed in both platelets and macrophages. However, the roles and function of $P2Y_{12/13}$ in the regulation of macrophage-mediated innate immune responses remain unclear. Here, we demonstrate that adenosine 5′-diphosphate (ADP), the endogenous ligand of $P2Y_1$, $P2Y_{12}$ and $P2Y_{13}$, was released both in *E. coli*-infected mice and from macrophages treated with either lipopolysaccharide (LPS) or Pam3CSK4. Furthermore, the expression of $P2Y_{13}$ was clearly increased in both LPS-treated macrophages and tuberculosis patients. ADP protected mice from *E. coli* 0111-induced peritonitis by recruiting more macrophages to the infected sites. Consistent with this, ADP and ADP-treated cell culture medium attracted more macrophages in the transwell assay by enhancing the expression of MCP-1. Nevertheless, $P2Y_1$ is dispensable for ADP-mediated protection against bacterial infection. However, either $P2Y_{12}$/$P2Y_{13}$ deficiency or blocking the downstream signaling of $P2Y_{12}$/$P2Y_{13}$ blocked the ADP-mediated immune response and allowed more bacteria to persist in the infected mice. Furthermore, extracellular signal-regulated kinase (ERK) phosphorylation was clearly increased by ADP, and this type of activation could be blocked by either forskolin or analogs of cyclic AMP (cAMP) (for example, 8-bromo-cAMP). Accordingly, ADP-induced MCP-1 production and protection against bacterial infection could also be reduced by U0126, forskolin and 8-bromo-cAMP. Overall, our study reveals a relationship between danger signals and innate immune responses, which suggests the potential therapeutic significance of ADP-mediated purinergic signaling in infectious diseases.
Cellular & Molecular Immunology (2018) **15,** 58–73; doi:10.1038/cmi.2016.56; published online 21 November 2016

Keywords: ADP; cAMP; danger signal; MCP-1; purinergic receptors

INTRODUCTION

As the first defense against invading pathogens, the innate immune system can be activated by pathogen-associated molecular patterns (PAMPs) through pattern-recognition receptors (PRRs), including toll-like receptors (TLRs), nucleotide-binding domain and leucine-rich repeat-containing receptors (NLRs) and RIG-I-like receptors (RLRs).[1,2] Increasing evidence has shown that danger-associated molecular patterns (DAMPs) such as high mobility group box 1 (HMGB1), heat shock proteins (HSPs), uric acid and nucleotides are all involved in the regulation of innate immune responses to abnormal cell death, stress and even microbial invasion.[3–5] Among these molecules, extracellular nucleotides, as the endogenous ligands of purinergic receptors, have been found to have great potential in the regulation of both physiological and pathological processes. In contrast to the extensively studied PRRs, the functions and mechanism of DAMPs in the innate immune response remain unclear.

Extracellular nucleotides, including adenosine 5′-triphosphate (ATP), adenosine 5′-diphosphate (ADP) and uridine-5′-diphosphate (UDP), can modulate the function of cells through ligand-gated ion channels (P2X) or G protein-coupled receptors (P2Y).[4,6] For example, ATP released from infected or stressed cells serves as an important danger signal that induces specific immune responses by activating P2X7. ATP triggers chemotactic mediator production by neutrophils, and autocrine signaling through the $P2Y_2$ receptor regulates the chemotaxis of these cells.[7] The activation of the NLRP3 inflammasome, which triggers the activation of inflammatory caspases, is conducted through ATP and activation of

Shanghai Key Laboratory of Regulatory Biology, Institute of Biomedical Sciences and School of Life Sciences, East China Normal University, Shanghai, China
[1]These authors contributed equally to this work.
Correspondence: Dr B Du, Shanghai Key Laboratory of Regulatory Biology, Institute of Biomedical Sciences and School of Life Sciences, East China Normal University, 500 Dongchuan Road, Shanghai 200241, China.
E-mail: bdu.ecnu@gmail.com
Received: 26 June 2016; Revised: 16 August 2016; Accepted: 16 August 2016

purinergic receptors.[8,9] Our previous study also showed that TLR-induced calcium mobilization protects mice against bacterial infection through extracellular ATP release.[10] However, the released ATP is highly volatile and can be rapidly hydrolyzed to ADP by CD39 to maintain the concentration of extracellular ADP at a high level.[11,12] Furthermore, platelet-dense granules are a source of ADP. In addition, the purinergic receptors $P2Y_{12}$ and $P2Y_{13}$ are highly expressed in platelets. Thus, previous studies of ADP and its receptors have focused mainly on blood clots that lead to stroke or heart attack as well as other vascular events. Interestingly, ADP and $P2Y_{12}$ receptor variants were shown to correlate with pulmonary inflammation and asthma.[13] However, although the level and expression of both extracellular ADP and its target receptors, respectively, are increased in bacterial infection, the function and mechanism of ADP and its receptors remain unknown.

The most extensively used treatment for bacterial infection is antibiotics such as cephalosporin, fluoroquinolone and trimethoprim-sulfamethoxazole. However, the widespread application of antibiotics also leads to resistance to these compounds, which is responsible for treatment failure.[14] The development of multidrug-resistant (MDR) bacterial strains is also considerable.[15] Owing to the severity of the growth of antimicrobial resistance, it is essential to further explore other mechanisms of host defense against bacterial infections, which will lay a theoretical foundation for immunoregulatory-based antibacterial therapies. Here, we demonstrate that both extracellular ADP and the expression of its receptors are enhanced during bacterial infection. In addition, extracellular ADP enhances MCP-1-mediated monocyte recruitment both *in vitro* and *in vivo*, which increases the clearance of invading pathogens and ameliorates mortality in a peritonitis mouse model through the activation of $G_{\alpha i}$-coupled P2Y receptors. Furthermore, we also provide evidence that increased intracellular cyclic AMP (cAMP) significantly blocks the ADP-dependent activation of the extracellular signal-related kinase (ERK) signaling pathway, which in turn is associated with MCP-1 production. Taken together, our findings demonstrate that extracellular ADP is an endogenous immune regulator that up-regulates host defense against bacterial infections through a cAMP-dependent signaling pathway.

MATERIALS AND METHODS

Reagents

Dulbecco's modified Eagle's medium (DMEM), fetal bovine serum (FBS), penicillin–streptomycin, Pam3CSK4 and TRIzol reagent were purchased from Life Technologies (Carlsbad, CA, USA). SYBR Premix Ex Taq and PrimeScript RT Master Mix were obtained from Takara (Dalian, China). Lipopolysaccharide (LPS), MRS2179, forskolin, 8-bromo-cAMP and ADP were acquired from Sigma-Aldrich (St Louis, MO, USA) and U0126 was purchased from Calbiochem (Temecula, CA, USA). Recombinant apyrase was acquired from New England Biolabs (Ipswich, MA, USA). The Mouse MCP-1 ELISA Kit and FITC anti-mouse CD11b, APC anti-mouse F4/80 and APC anti-mouse Ly6G antibodies were obtained from BioLegend (San Diego, CA, USA). The ADP Colorimetric/Fluorometric Assay Kit was purchased from Sigma-Aldrich (St Louis, MO, USA). Antibodies specific to GAPDH, p38, phosphorylated p38, JNK, phosphorylated JNK, MEK1/2, phosphorylated MEK1/2, ERK and phosphorylated ERK were acquired from Cell Signaling Technology (Boston, MA, USA). AlexaFluor 680 secondary antibodies were purchased from Jackson ImmunoResearch (West Grove, PA, USA).

Ethics statement

All animal experiments conformed to the regulations drafted by the Association for Assessment and Accreditation of Laboratory Animal Care in Shanghai and were in direct accordance with the guidelines from the Ministry of Science and Technology of the People's Republic of China on Animal Care. The protocol was approved by the East China Normal University Center for Animal Research (AR2013/08002). All surgeries were performed under anesthesia, and all efforts were made to minimize suffering. The clinical data were collected from the GEO Profile Database (http://www.ncbi.nlm.nih.gov/geoprofiles, NCBI, NIH). The work was approved by the Institutional Review Board of Shenzhen Third People's Hospital.[16]

Animals

For primary macrophage isolation and the peritonitis mouse model, female C57BL/6 mice (6–8 weeks old) were purchased from the Shanghai Laboratory Animal Company (Shanghai, China). $P2Y_{12}{}^{-/-}$ mice on a C57BL/6 background were a kind gift from Prof. Junling Liu. $P2Y_1{}^{-/-}$ and $P2Y_{13}{}^{-/-}$ mice on a C57BL/6 background were generated using a CRISPR/Cas9 system at the Laboratory Animal Center of East China Normal University (Shanghai, China). RNA products that contained specific target sequences were purified and injected into C57BL/6 mouse zygotes. The F0 mice were identified by T7E1 mismatch-sensitive assays. The sequence of the target site for mouse $P2Y_1$ was 5′-CGGGCCTGGGCTCGCTTTGGG-3′, and target site for mouse $P2Y_{13}$ was 5′-CGGTGCCCAGGG ACACTCGG-3′. The Cas9 endonuclease-mediated genome editing led to a random insertion of 290 bp ($P2Y_1$) or deletion of 307 bp ($P2Y_{13}$) between sites, which contributed to the loss of function of mouse $P2Y_1$ and $P2Y_{13}$, respectively. Primer sequences for the identification of $P2Y_1{}^{-/-}$ mice were 5′-CGCACGTCCTTCAGCTTAGA-3′ (sense) and 5′-ACACC AGCACGCTGACATAA-3′ (antisense), and for the identification of $P2Y_{13}{}^{-/-}$ mice were 5′-TCAAATCCGCTGAATGAGTT-3′ (sense) and 5′-ACTCTTCAAAGATGCACT-3′ (antisense). All mice used in these experiments were housed in pathogen-free conditions and were maintained in accordance with the institutional guidelines (Laboratory Animal Center, East China Normal University).

Cell culture

The mouse cell line RAW 264.7 was obtained from the American Type Culture Collection (ATCC, USA) and cultured in DMEM containing 10% FBS, 100 U/ml penicillin and 100 mg/ml streptomycin. The cells were incubated in a 5%

CO_2 incubator at 37 °C. Bone marrow-derived macrophages (BMDMs) and peritoneal macrophages (PEMs) were obtained as previously described.[17] The generated BMDMs and PEMs were F4/80$^+$ (purity, 90%).

ADP assay

RAW 264.7 cells (5×10^4 cells per well) were seeded in 24-well plates (Corning Costar, Corning, NY, USA) and then starved in serum-free DMEM for 12 h before the ADP assay. Either LPS or Pam3CSK4 was added at the time points indicated. Then, the collected supernatants were used to quantify the extracellular ADP using the ADP Colorimetric/Fluorometric Assay Kit (Sigma-Aldrich) as the manufacturer's instructions. The ADP levels were calculated based on an ADP standard curve. For ADP detection *in vivo*, the peritoneal fluid was collected from *E. coli* 0111-injected mice at different time points, and the level of ADP in the peritoneal fluid was assayed as described above. All samples were measured in triplicate, and all experiments were repeated at least three times.

RNA isolation and real-time polymerase chain reaction

BMDMs, PEMs and RAW 264.7 cells were stimulated with different concentrations of ADP for 3 h, and total RNA was isolated using TRIzol reagent (Life Technologies) according to the manufacturer's protocol. Complementary DNA as synthesized with 500 ng RNA using a reverse transcription kit (Takara) according to the manufacturer's instructions and then used for real-time (RT)-quantitative polymerase chain reaction (qPCR) analysis with SYBR Premix Ex Taq (Takara). The data were analyzed using the Stratagene Mx3005P Real-Time qPCR System (Agilent Technologies, Santa Clara, CA, USA). The housekeeping genes *β-actin* and *GAPDH* were used to normalize the transcriptional levels of target genes, and the relative expression was calculated using the $\Delta\Delta C_t$ method. The sequence-specific primers are listed in Table 1.

MCP-1 measured by enzyme-linked immunosorbent assay

To assay the secretion of MCP-1, RAW 264.7 cells were seeded in 12-well plates (Corning Costar) at 5×10^4 per well and cultured in DMEM overnight. Then, the cells were pretreated with drugs as indicated. After stimulation with ADP for an additional 24 h using phosphate-buffered solution (PBS) as a negative control, the supernatants were centrifuged for 5 min. The production of MCP-1 was measured using a Mouse MCP-1 ELISA kit (BioLegend).

Transwell migration assay

RAW 264.7 cells (1×10^5 cells per well) or PEMs (2×10^5 cells per well) suspended in serum-free DMEM were added onto the upper well of a 24-well transwell insert with an 8 μm polycarbonate membrane (Falcon, Durham, NC, USA), and the bottom well was supplemented with ADP-treated culture medium. After 8 h of migration, the insert membranes were gently scraped with a cotton swab to remove the residual cells, and then the cells in the lower membrane that had migrated were fixed with 4% paraformaldehyde. Finally, Giemsa staining was conducted to count the cells using an optical microscope (Leica, Wetzlar, Germany) at 200× magnification.

Western blotting

Cells were seeded in 6-well plates (Corning Costar) and stimulated with ADP at the times indicated. The samples were separated by 10% SDS-PAGE and transferred to polyvinylidene fluoride (PVDF) membranes (Millipore, Boston, MA, USA). After incubation with phospho-protein kinase A (PKA), PKA, phospho-ERK1/2, ERK1/2, phospho-p38, p38 and phospho-JNK, MEK1/2 or phospho-MEK1/2 antibodies, the PVDF membranes were then incubated with the appropriate AlexaFluor 680 secondary antibodies. Finally, a Li-COR Odyssey imaging system (Lincoln, NE, USA) was used to detect the proteins.

Table 1 Sequence-specific primer list

Gene name	*Primers (5′–3′)*	*Size/bp*
$P2Y_1$	Sense: TACAATGACCTGGACAACT	95
	Antisense: GTTACCTGATAAGTGGCATAA	
$P2Y_{12}$	Sense: AACTCTATCGGTCTTATGTCA	191
	Antisense: AGAATACAGCAATGATGATGAA	
$P2Y_{13}$	Sense: GCTGGAGGTGAAGGTATT	87
	Antisense: CTGTAAGTGTATGGTATTCTGAC	
MCP-1/CCL-2	Sense: TTAAAAACCTGGATCGGAACCAA	121
	Antisense: GCATTAGCTTCAGATTTACGGGT	
CCL-3	Sense: TTCTCTGTACCATGACACTCTGC	100
	Antisense: CGTGGAATCTTCCGGCTGTAG	
CCL-4	Sense: TTCCTGCTGTTTCTCTTACACCT	121
	Antisense: CTGTCTGCCTCTTTTGGTCAG	
β-Actin	Sense: AGTGTGACGTTGACATCCGT	298
	Antisense: GCAGCTCAGTAACAGTCCGC	
GAPDH	Sense: AGGTCGGTGTGAACGGATTTG	123
	Antisense: TGTAGACCATGTAGTTGAGGTCA	

Proliferation assay of bacteria

A single colony from an *E. coli* 0111:B4 plate was loaded into 5 ml of LB liquid medium in a shaker at 200 rpm and 37 °C for 16 h, and the bacteria suspension culture was then diluted 1:100 for another 2 h vigorous shaking to prepare the *E. coli* for the log phase. Then, the *E. coli* was treated with 0, 100, 500, 1000, of 5000 μM ADP for 12 h, and bacteria were diluted and cultured on solid LB agar medium. Single colony-forming units (CFUs) were counted to determine the proliferation of the bacteria.

Peritonitis mouse model

Wild-type (WT), $P2Y_{12}^{-/-}$ and $P2Y_{13}^{-/-}$ C57BL/6J female mice (6–8 weeks old) were chosen to induce peritonitis to mimic bacterial infection. The peritoneal bacterial load and survival curves were obtained to reflect the protective effect of ADP. For *E. coli* 0111 counting in the peritoneal fluid, the mice were randomly divided into several groups and pretreated with an intraperitoneal (i.p.) injection of PBS, ADP (50 mg/kg) or apyrase (100 U/kg). After 12 h, each mouse was challenged with *E. coli* 0111 via i.p. injection. After 12 h, the *E. coli* were lavaged with 2 ml PBS from the abdominal cavities of the mice and diluted ten times in PBS, and 20 μl of the bacterial suspension was cultured on solid LB agar medium for 12 h. The single CFUs were counted to determine the quantity of *E. coli* in the peritoneal fluid. The other groups were divided and treated as described above. Instead of counting the *E. coli* in the peritoneal fluid, the mice were checked every 2 h to obtain a survival curve.

Flow cytometry

Cells were harvested from the peritoneal fluid that was collected as described above. They were washed with staining buffer and then incubated with FITC anti-mouse CD11b and either APC anti-mouse F4/80 (macrophage) or APC anti-mouse Ly6G (neutrophil) monoclonal antibodies (BioLegend) in 50 μl of staining buffer for 30 min. Cells were washed twice and resuspended in 200 μl of staining buffer and then analyzed on a FACSCalibur flow cytometer (BD Biosciences).

Statistical analysis

The data are presented as the mean ± s.e.m. ($n = 3$–6). Statistical significance was evaluated with Student's *t*-test or one-way ANOVA followed by the Dunnett's multiple comparison. The *P*-values < 0.05, < 0.01 and < 0.001 indicated a significant difference between the groups. For the survival curve analysis, the log-rank test was performed, and a *P*-value < 0.05 is considered statistically significant.

RESULTS

The levels of extracellular ADP and its receptors are highly correlated with bacterial infection

The release of intercellular nucleotides initiates the activation of purinergic receptors as a danger signal. Thus, to evaluate the potential regulation of ADP during bacterial infection, extracellular ADP (eADP) was measured using a colorimetric assay in both *E. coli*-infected mice and either LPS (TLR4 agonist)- or Pam3CSK4 (TLR 1/2 agonist)-treated macrophages. As shown in Figure 1a, the eADP levels in the peritoneal cavities of mice challenged with *E. coli* 0111 were increased in a time-dependent manner. Furthermore, a similar increase in eADP was also observed in cells treated with either LPS (Figures 1b and c) or Pam3CSK4 (Figures 1d and e). In addition, the expression of $P2Y_{13}$ (an ADP receptor) was also markedly enhanced in tuberculosis patients (Figure 1f) as well as in LPS-treated RAW 264.7 cells (Figure 1g) and BMDMs (Figure 1h). These data demonstrate the great potential of ADP-associated signaling in bacterial infection.

Extracellular ADP enhances host defense against invading bacteria by recruiting more monocytes

To investigate the potential role of eADP in host defense against invading bacteria, we established a peritonitis mouse model using an i.p. injection of *E. coli* 0111 to monitor bacterial clearance and mouse survival. As shown in Figure 2a, the survival of ADP-treated mice was clearly increased, and the ADP-mediated protection could be eliminated by treatment with apyrase, which hydrolyzes ADP into adenosine. Accordingly, the total quantity of bacteria in the peritoneal cavity was reduced in ADP-injected mice, and this type of protection could also be blocked by apyrase (Figure 2b). However, the proliferation of bacteria was minimally influenced by ADP (Figure 2c), suggesting that the ADP-mediated protection occurred mainly through the regulation of host defenses. Furthermore, the invading bacteria were clearly reduced whenever the mice were treated with ADP either before or after the establishment of the infection (Figure 2d). Accordingly, the invading bacteria were significantly increased whenever the mice were treated with apyrase either before or after the establishment of the infection (Figure 2e). Consequently, the total cell and leukocyte numbers in the abdominal cavities of ADP-treated mice were both much higher than in the control group (Figures 3a and b). Furthermore, macrophages in the peritoneal cavities of ADP-treated mice were also significantly increased (Figure 3c). However, neutrophils, which have an important role in defense against bacterial infection, were minimally influenced by ADP (Figure 3d). Thus, our data suggest that ADP may protect bacterially infected mice by recruiting more macrophages.

The migration of macrophages is enhanced by ADP-treated cell supernatants

The recruitment of innate immune cells to infected sites is the first step in fighting against invading pathogens. For this reason, we established a transwell migration assay to investigate the role of ADP in the regulation of cell motility. As shown in Figure 4a, when we added ADP-treated cell supernatants into the lower chamber for 8 h, the migration of RAW 264.7 cells was markedly increased. To determine the effect of extracellular ADP on migration, the supernatant-induced cell migration was minimally altered by apyrase (which hydrolyzed the nucleotides in

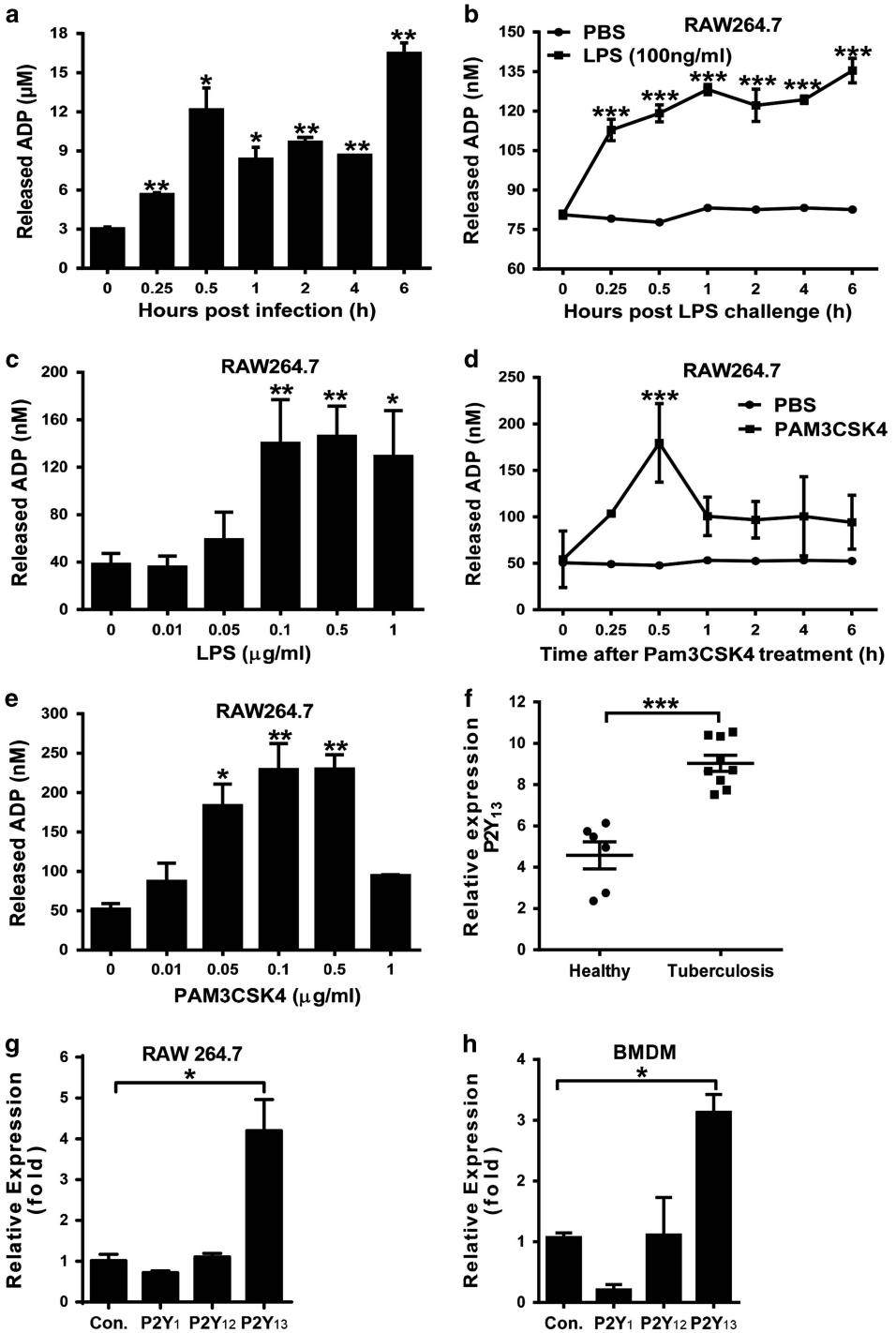

Figure 1 Bacterial infection enhances ADP release and $P2Y_{12}$/$P2Y_{13}$ expression in macrophages. (**a**) *E. coli* 0111 (2×10^8 CFU) was injected into the abdominal cavities of mice. Then, eADP was detected using an ADP colorimetric assay at different time points, and the concentration of ADP was calculated according to a standard curve. The quantification of eADP is shown for the macrophage cell line RAW 264.7 treated with either (**b**) 100 ng/ml LPS for different time periods or (**c**) different doses of LPS. Measurement of eADP in the macrophage cell line RAW 264.7 treated with either (**d**) 100 ng/ml Pam3CSK4 for different time periods or (**e**) different doses of Pam3CSK4. (**f**) Relative mRNA expression of $P2Y_{13}$ in peripheral mononuclear cells from tuberculosis patients ($n=9$). The clinical data were collected from the GEO Profile Database (http://www.ncbi.nlm.nih.gov/geoprofiles, NCBI, NIH). Quantitative PCR assays for $P2Y_1$, $P2Y_{12}$ and $P2Y_{13}$ mRNA expression levels in (**g**) the macrophage cell line RAW 264.7 and (**h**) BMDMs incubated with 100 ng/ml LPS for 3 h. The relative expression was calculated using the $\Delta\Delta C_t$ method. All values are expressed as the mean ± s.e.m., and each experiment was independently performed three times. Statistical analysis was performed with one-way ANOVA (**a**–**e**, **g**, **h**) or Student's *t*-test (**f**); $^*P<0.05$, $^{**}P<0.01$, $^{***}P<0.001$. ADP, adenosine 5′-diphosphate; eADP, extracellular ADP.

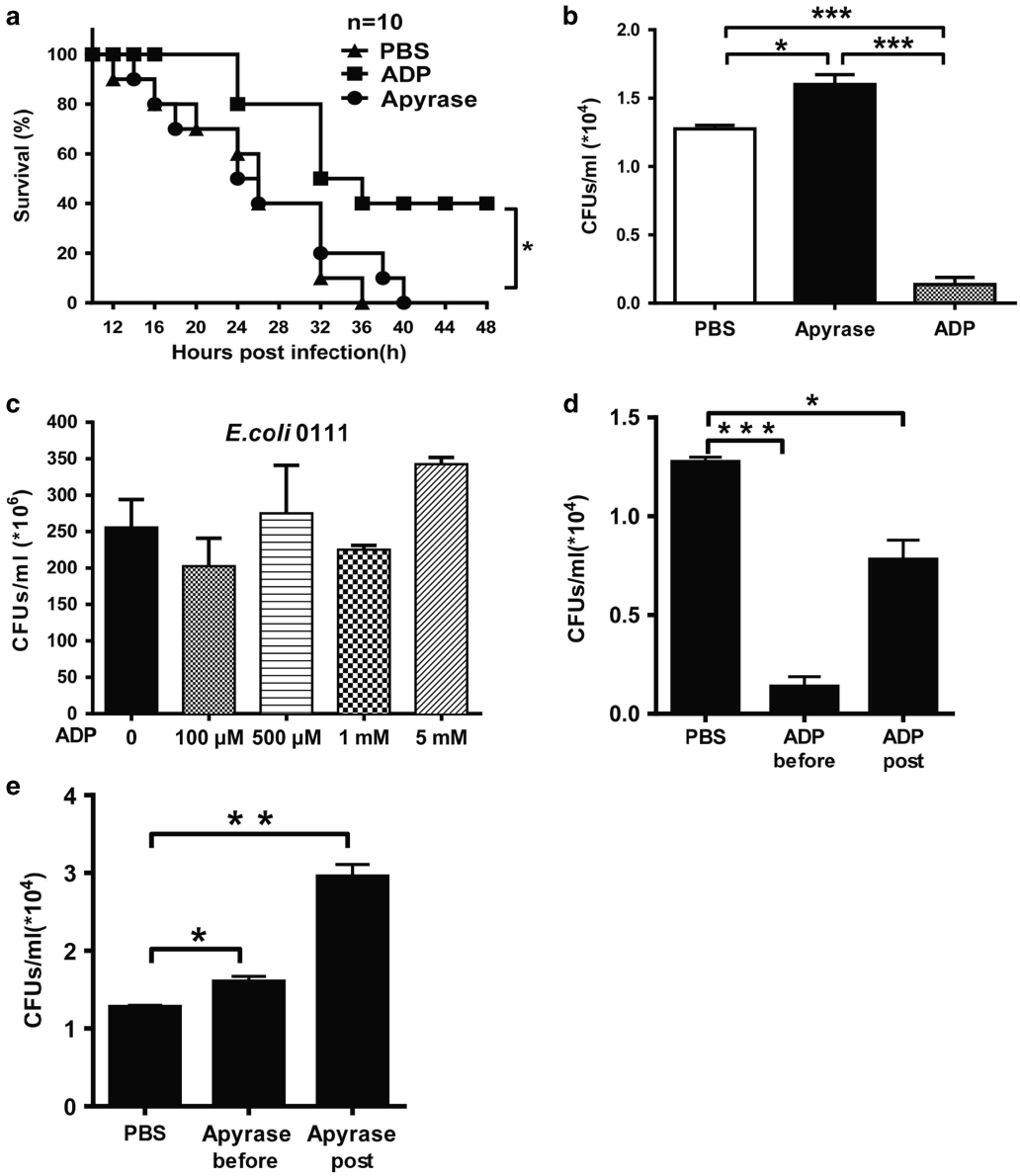

Figure 2 ADP enhances host defense against invading bacteria in a peritonitis mouse model. C57BL/6J mice were challenged by an i.p. injection of PBS, ADP (50 mg/kg) or apyrase (100 U/kg) before they were infected with *E. coli* 0111 (1×10^8 CFU). (**a**) Twelve hours after i.p. injection of *E. coli*, the surviving mice were monitored every 2 h over the next 48 h ($n=10$ mice per group). (**b**) After 12 h, the peritoneal fluid was lavaged with 3 ml PBS and then diluted 10-fold in PBS, and the bacterial counts were determined by plating on solid LB agar plates ($n=6$ mice per group). (**c**) The concentration of *E. coli* was treated with different doses of ADP as shown, and then the bacteria were cultured in solid LB agar media for 12 h. WT mice received an i.p. injection of PBS, ADP (100 μM) (**d**) or apyrase (**e**) as indicated before or after infection with 1×10^8 CFU of *E. coli* 0111 ($n=4$–5 mice per group). Twelve hours after i.p. injection of *E. coli*, the peritoneal fluid was lavaged with 3 ml of PBS and diluted 10-fold in PBS, and the bacterial counts were determined by plating on solid LB agar plates. All values are expressed as the mean ± s.e.m., and each experiment was independently performed three times. Statistical analysis was performed with the log-rank test (**a**) and two-tail unpaired Student's *t*-test (**b**–**e**). Significant differences between groups were represented as $^*P<0.05$. ADP, adenosine 5′-diphosphate; PBS, phosphate-buffered solution; i.p., intraperitoneal; WT, wild-type. $^{**}P<0.01$ and $^{***}P<0.001$

the supernatant), suggesting that the extracellular nucleotides were dispensable in the recruitment of macrophages. Similar data were also observed for the recruitment of PEMs by ADP-treated cell supernatants (Figure 4b).

ADP-enhanced cell migration occurs mainly through MCP-1 production

The chemokines released during the immune response can recruit immune cells, which have important roles in fighting

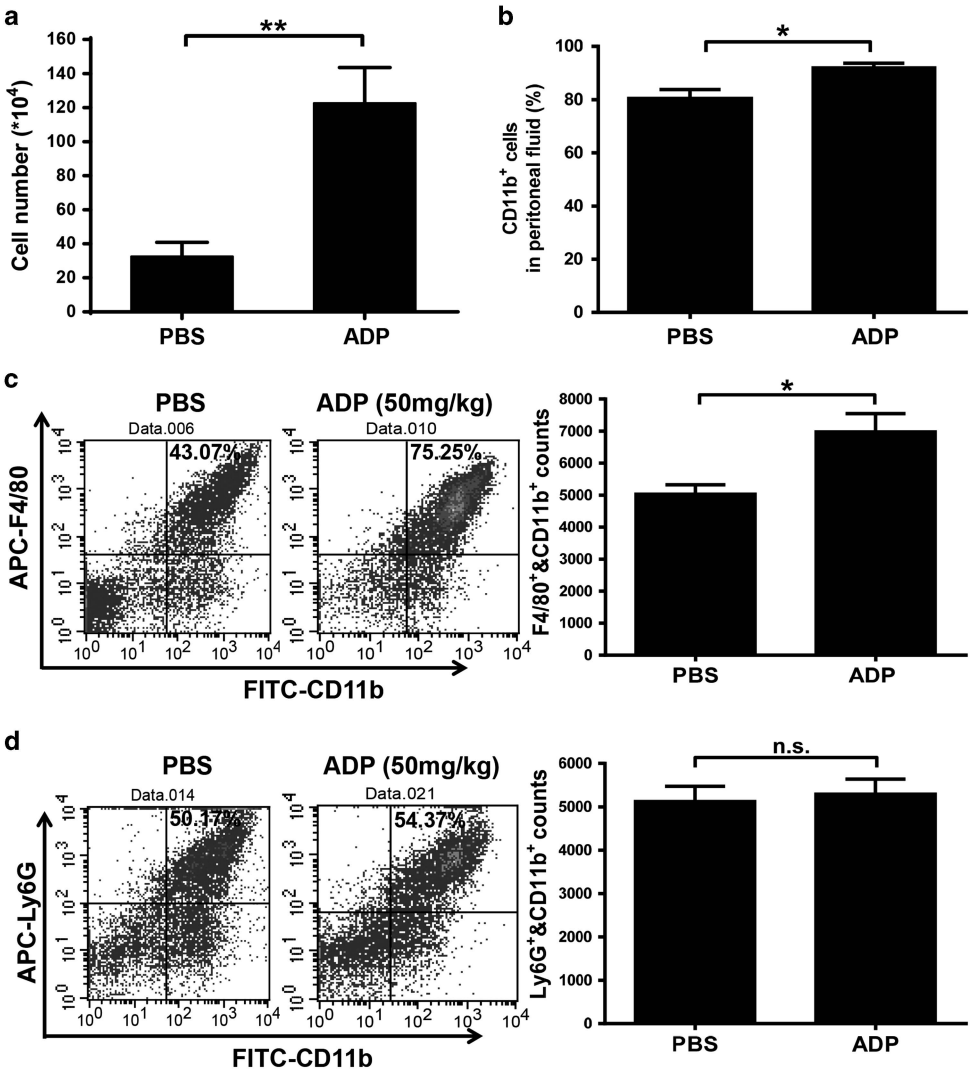

Figure 3 ADP promotes macrophage recruitment to the bacterially infected abdominal cavity. Mice received an i.p. injection of PBS or ADP (50 mg/kg) as indicated before infection with 1×10^8 CFU of *E. coli* 0111 ($n=4$–5 per group). Then, the cells present in the abdominal cavity were harvested at 12 h. (**a**) The leukocyte counts of the peritoneal fluid were processed by light microscopy. Flow cytometric analysis was performed with peritoneal leukocytes injected with PBS and ADP (50 mg/kg) before *E. coli* 0111 infection and collected 12 h after inoculation. The percentage, counts and representative dot plots of infiltrating myeloid cells (**b**), macrophages ($CD11b^+$, $F4/80^+$) (**c**) and neutrophils ($CD11b^+$, $Ly6G^+$) (**d**) are shown. The values are expressed as the mean ± s.e.m., and each experiment was independently performed three times with 4–5 mice per group as shown. Statistical analysis was performed with Student's *t*-test; $^*P<0.05$, $^{**}P<0.01$. ADP, adenosine 5′-diphosphate; PBS, phosphate-buffered solution; i.p., intraperitoneal.

against invading pathogens, to the infected sites. To explore the key components involved in ADP-enhanced cell migration, we measured the expression of different chemokines in ADP-treated mice and macrophages. As shown in Figure 5a, only the RNA expression of MCP-1 (CCL-2) was clearly increased in ADP-treated RAW 264.7 cells. In addition, the protein level of MCP-1 was also increased in the lavage fluid of the abdominal cavities of ADP-treated mice (Figure 5b). Accordingly, ADP significantly increased the production of MCP-1 in RAW 264.7 cells in both a time-dependent (Figure 5c) and dose-dependent (Figure 5d) manner. Consequently, if we blocked the function of MCP-1 with an MCP-1-specific antibody, the ADP-increased cell migration was restored to basal levels, suggesting that the ADP-mediated recruitment of immune cells occurs mainly through MCP-1 (Figure 5e).

$P2Y_1$ is dispensable for ADP-mediated protection against bacterial infection

It has been shown that ADP can activate the $P2Y_1$, $P2Y_{12}$ and $P2Y_{13}$ receptors, which modulate downstream signaling through their $G_{\alpha q}$ ($P2Y_1$) and $G_{\alpha i}$ subunits ($P2Y_{12}$, $P2Y_{13}$). Thus, to explore the potential signaling involved in ADP-induced MCP-1 production, we treated mice with ADP and MRS2179 (a specific antagonist of $P2Y_1$). As shown in

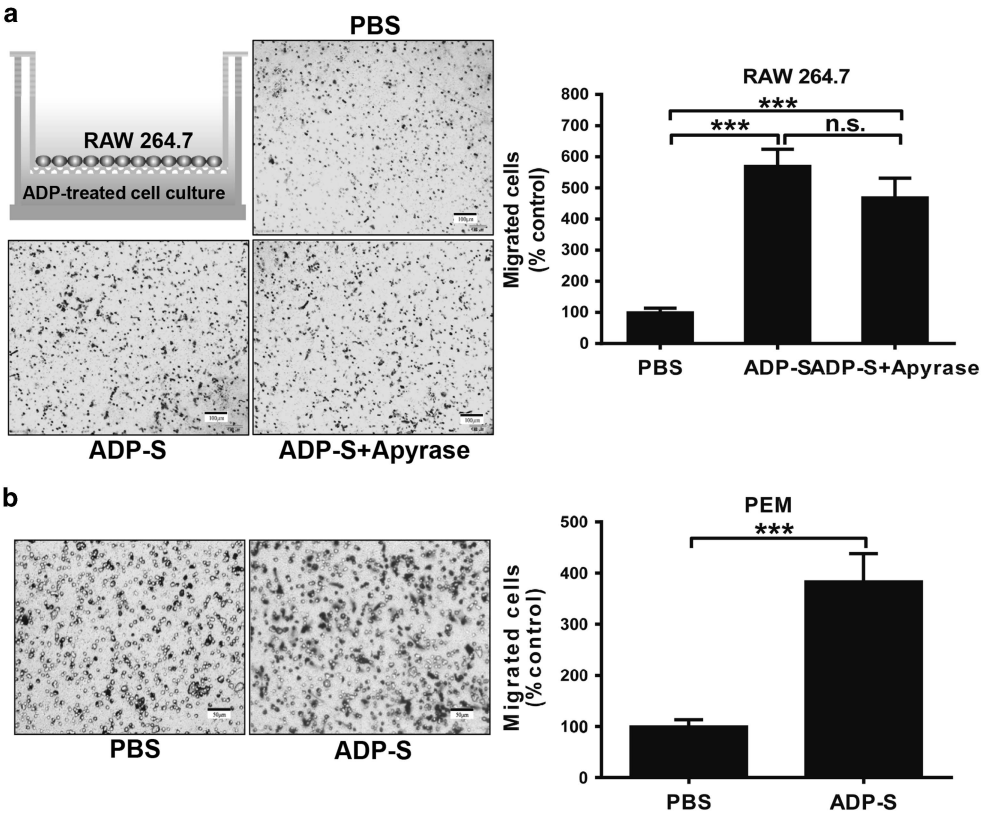

Figure 4 ADP-treated cell supernatants attract the migration of macrophages in a transwell chamber assay. (**a**) RAW 264.7 cells were treated with ADP (100 μM) or PBS (control) for 12 h, and then the supernatants from ADP-treated cells (ADP-S) were incubated with apyrase (1 U/ml) and collected for a transwell assay. After incubating for 8 h at 37 °C, the migrating cells on the filter were stained with Giemsa reagent, and their counts were normalized to the number of migrating control cells incubated with PBS. (**b**) In addition, ADP-treated cell supernatants were used in a chemotaxis assay with PEMs as described above. Representative pictures and statistical results are shown. Scale bar = 100 μm (**a**) and 50 μm (**b**). The data are presented as the mean ± s.e.m., and statistical analysis was performed with one-way ANOVA (**a**) or Student's *t*-test (**b**). ***$P<0.001$ indicate significant differences between groups; representative data from one of three independent experiments are shown. ADP, adenosine 5′-diphosphate; PBS, phosphate-buffered solution; PEM, peritoneal macrophage.

Figure 6a, the survival of the bacterially infected mice was markedly increased by ADP, and this type of protection could not be blocked by the $P2Y_1$ inhibitor MRS2179. The ADP-mediated reduction in the bacterial load was also not blocked by MRS2179 (Figure 6b). Similarly, the ADP-mediated increases in macrophage recruitment (Figure 6c) and MCP-1 production (Figure 6d) were minimally affected by MRS2179. Furthermore, the production of MCP-1 was clearly increased by ADP in $P2Y_1$ knockout mice, implying that $P2Y_1$ is dispensable for ADP-mediated protection against bacterial infection.

$P2Y_{12}$ and $P2Y_{13}$ are both involved in ADP-mediated immune regulation

To further illuminate the mechanism involved in ADP-mediated immune responses, we established both $P2Y_{12}$ and $P2Y_{13}$ knockout mice using CRISPR/Cas9 (clustered regularly interspaced short palindromic repeats) technology. As shown in Figure 7a, the bacterial load in $P2Y_{12}$-deficient mice was minimally changed, but the bacterial load in ADP-treated $P2Y_{12}$ knockout mice was greater than that in the ADP-treated WT mice. However, the number bacteria in the $P2Y_{13}$ knockout mice were markedly increased, although ADP was still able to reduce the bacterial load in $P2Y_{13}$ knockout mice (Figure 7b). Furthermore, the number of recruited macrophages in the infected peritoneal fluid was clearly reduced in both $P2Y_{12}$ (Figure 7c) and $P2Y_{13}$ (Figure 7d) knockout mice. The ADP-enhanced MCP-1 production was also reduced in both $P2Y_{12}$ (Figure 7e) and $P2Y_{13}$ (Figure 7f) knockout macrophages. Consequently, the ADP-induced increase in MCP-1 production was eliminated in $P2Y_{12}$ and $P2Y_{13}$ double knockout mice, suggesting the dominant role of $P2Y_{12}$ and $P2Y_{13}$ in ADP-mediated immune regulation (Figure 7g). To further confirm the role of $P2Y_{12}$ and $P2Y_{13}$ in ADP-mediated protection, we pretreated $P2Y_{13}$ knockout mice with prasugrel (a $P2Y_{12}$ specific inhibitor) to mimic the phenotype of $P2Y_{12}$ and $P2Y_{13}$ double knockout mice. As shown in Figure 7h, the survival of bacterially infected WT mice was clearly increased by ADP. However, there is no significant difference was observed in prasugrel-treated P2Y13 knockout mice with or without ADP. These data suggest that $P2Y_{12}$ and $P2Y_{13}$ are both involved in ADP-mediated immune protection and that ADP-induced MCP-1 production and immune protection could be altered if only one of these receptors was deleted.

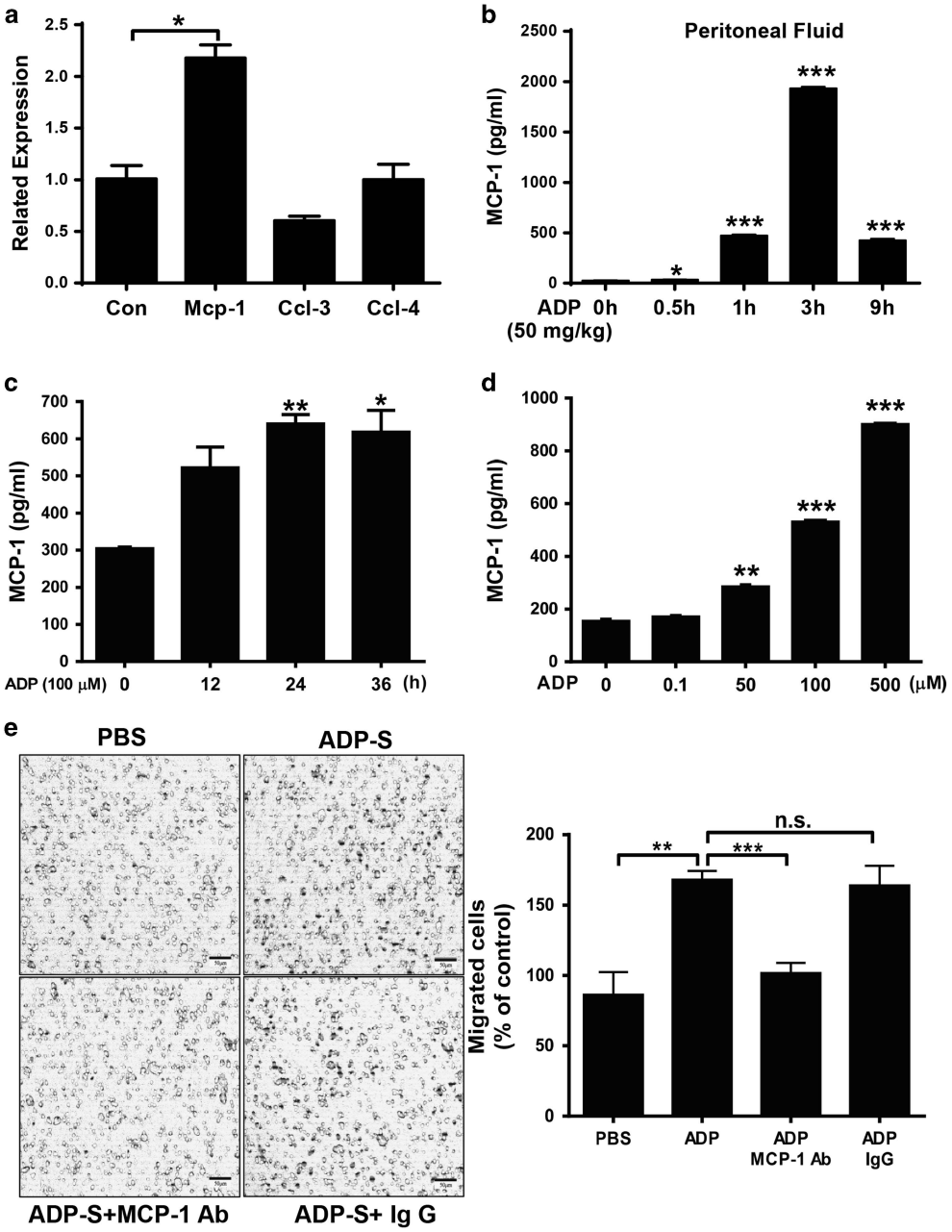

Figure 5 ADP-induced MCP-1 production is important for macrophage migration. (**a**) RAW 264.7 cells were stimulated with 100 μM ADP for 6 h. The mRNA levels of different chemokines, including MCP-1/CCL-2, CCL-3 and CCL-4, were analyzed by quantitative RT-PCR. Relative expression was calculated using the $\Delta\Delta C_t$ method. (**b**) The protein levels of MCP-1 were measured by enzyme-linked immunosorbent assay (ELISA) using supernatants obtained from abdominal cavity washes after ADP (50 mg/kg) injection. The MCP-1 protein level was quantified in the macrophage cell line RAW 264.7 treated with (**c**) 100 μM ADP for different time periods or (**d**) different doses of ADP. (**e**) RAW 264.7 cells were treated with 100 μM ADP, and the resulting cell supernatants (ADP-S) were used for a transwell assay. MCP-1 was added as a positive control, and an MCP-1 blocking Ab was also added to block MCP-1 activity in the ADP-treated cell supernatant. In addition, an unrelated mouse mAb (5 mg/ml) was used in this test. Scale bar = 50 μm. The data are presented as the mean ± s.e.m., and each experiment was independently performed three times. Statistical analysis was performed with one-way ANOVA; $^*P<0.05$, $^{**}P<0.01$, $^{***}P<0.001$. ADP, adenosine 5′-diphosphate; PBS, phosphate-buffered solution; RT-PCR, real-time polymerase chain reaction.

cAMP-regulated ERK phosphorylation is activated by ADP

To demonstrate the mechanism of ADP-induced MCP-1 production, we measured MCP-1-associated signaling using a western blot assay. As shown in Figure 8a, the phosphorylation of ERK was significantly increased by ADP in RAW 264.7 cells, whereas MEK, p38 and JNK were minimally affected. Similar data were also observed in BMDMs (Figure 8b). The phosphorylation of PKA was clearly decreased by ADP, implying

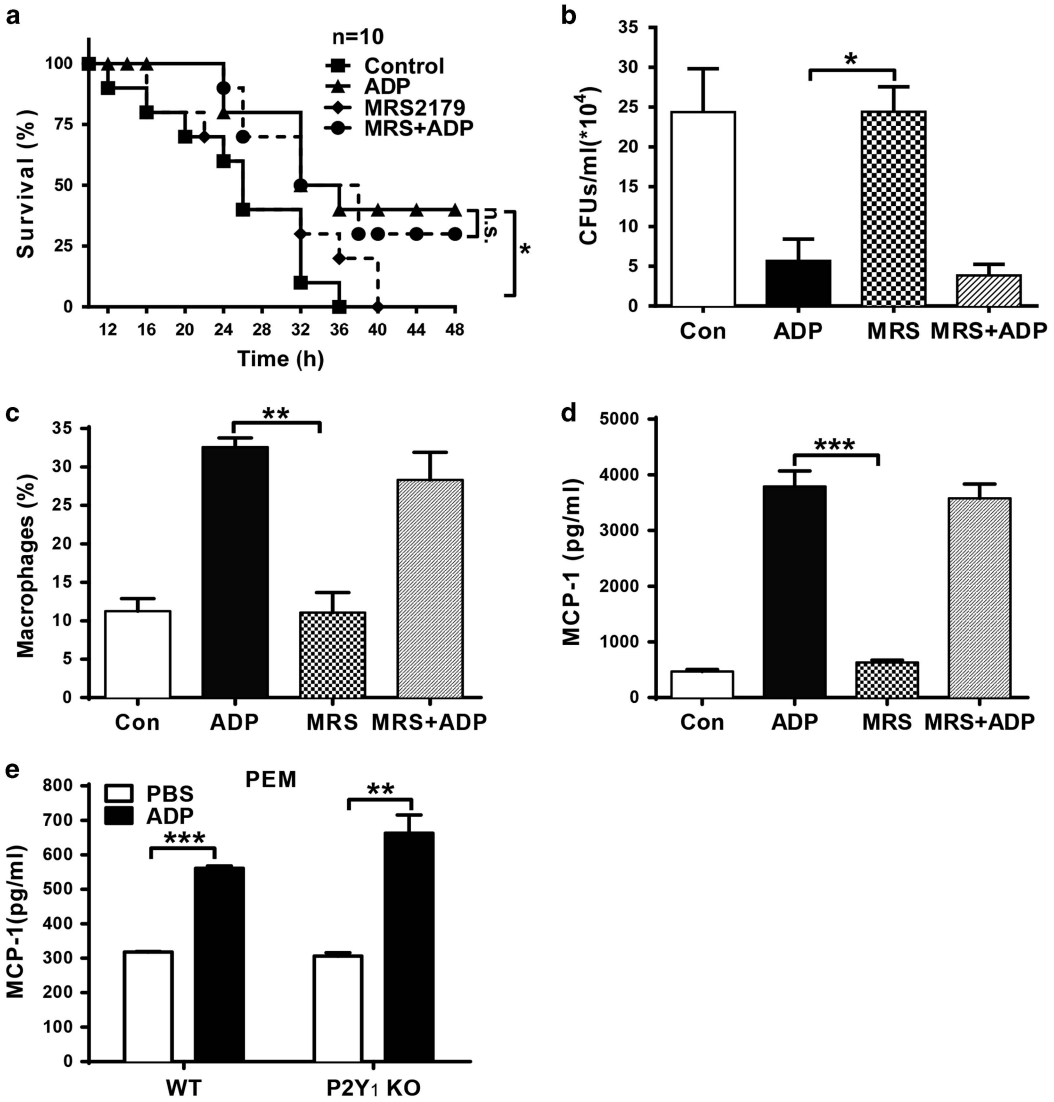

Figure 6 $P2Y_1$ is dispensable for ADP-mediated host defense against infection. Mice were pretreated with an injection of PBS, ADP (50 mg/kg), MRS2179 (MRS, 10 μM) or MRS2179, and ADP for 12 h before *E. coli* 0111 injection (1×10^8 CFU). (**a**) Twelve hours after the injection of *E. coli*, the survival of the mice was monitored every two hours over the next 48 h ($n=10$ mice per group). (**b**) After another 12 h, the peritoneal fluid was lavaged with 3 ml PBS and then diluted 10-fold in PBS, and the bacterial counts were determined by plating on solid LB agar plates. (**c**) The percentage of macrophages and (**d**) MCP-1 protein levels in the peritoneal fluid of the groups of mice were measured. (**e**) PEMs from WT and $P2Y_1^{-/-}$ mice were treated with the ADP (100 μM) for 24 h. Then, cell supernatants were harvested to detect the concentration of MCP-1 by ELISA. The results are presented as the mean ± s.e.m., and each experiment was independently performed three times. Statistical analysis was performed with the log-rank test (**a**) and either Student's *t*-test (**e**) or one-way ANOVA (**b**–**d**); $^*P<0.05$, $^{**}P<0.01$, $^{***}P<0.001$. ADP, adenosine 5′-diphosphate; PBS, phosphate-buffered solution; PEM, peritoneal macrophage, WT, wild-type.

crosstalk between ERK signaling and cAMP signaling (Figure 8c). When we pretreated cells with forskolin (an activator of adenylate cyclase) before ADP treatment, the ADP-mediated increase in ERK signaling was reduced to less than the normal increase observed after both forskolin and U0126 (a highly selective inhibitor of MEK1/2) treatment (Figure 8d). Furthermore, if we pretreated the cells with 8-Bromo-cAMP (a PKA activator), the ADP-enhanced ERK signaling was also significantly decreased. Taken together, these data demonstrate that the ADP-mediated increase in ERK activation occurs mainly through cAMP/PKA signaling.

ADP increases MCP-1 production through cAMP/PKA/ERK signaling

To further confirm the mechanism involved in ADP-mediated immune regulation, we used different inhibitors to investigate the role of the cAMP/PKA/ERK signaling axis. As shown in Figure 9a, the migration of RAW 264.7 cells was increased dramatically when exposed to ADP-treated cell supernatants. However, this increase returned to basal levels upon co-treatment with the ERK inhibitor U0126 (Figure 9a). Moreover, the recruitment of RAW 264.7 cells by ADP could also be inhibited by forskolin

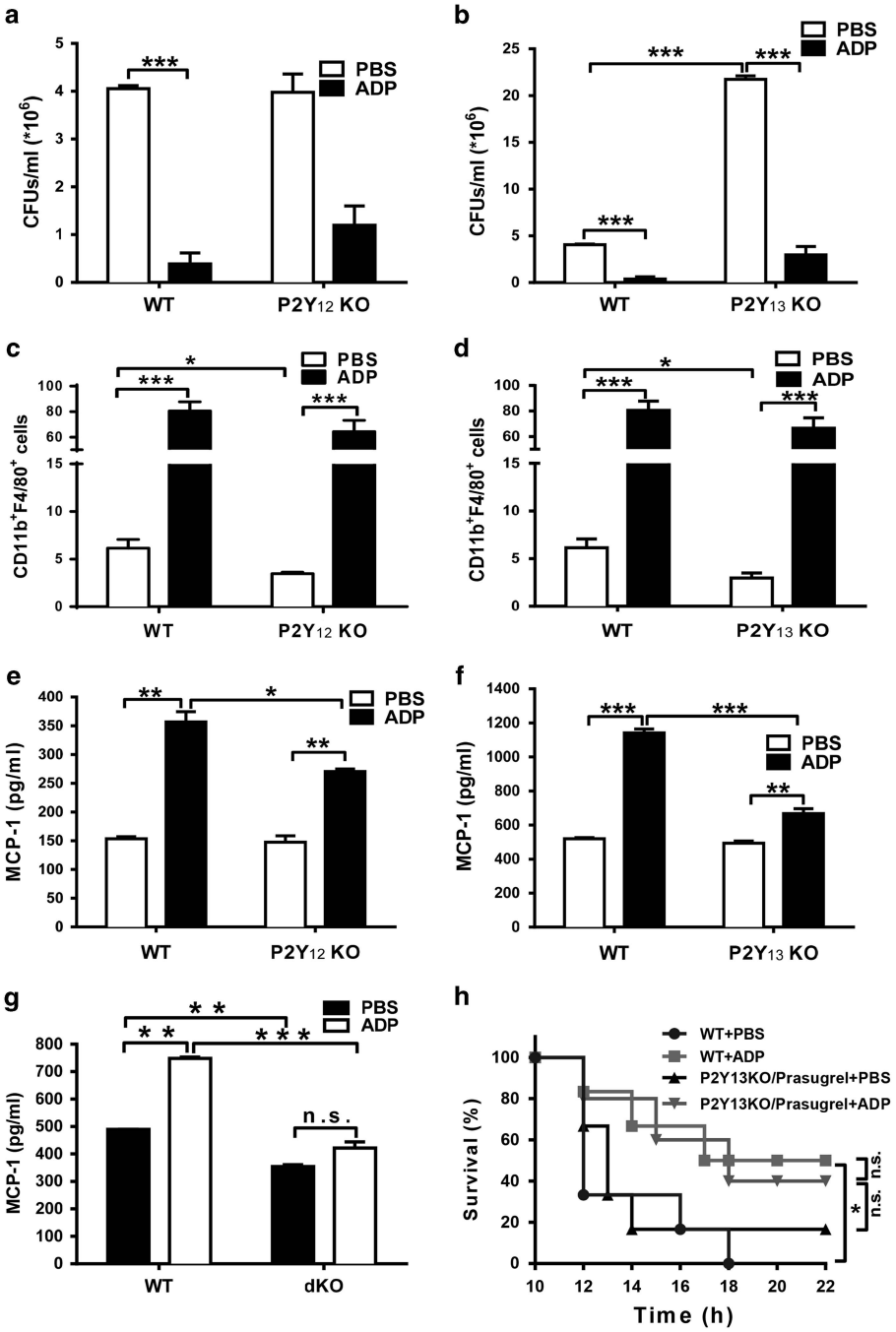

Figure 7 $P2Y_{13}$ is partly involved in ADP-induced MCP-1 production and macrophage recruitment. WT, (**a**) $P2Y_{12}$ knockout and (**b**) $P2Y_{13}$ knockout mice received an i.p. injection of PBS or ADP (100 μM) as indicated before infection with 1×10^8 CFU of *E. coli* 0111 ($n=4$–5 mice per group). Twelve hours after i.p. injection of *E. coli*, the peritoneal fluid was lavaged with 3 ml of PBS and diluted 10-fold in PBS, and the bacterial counts were determined by plating on solid LB agar plates ($n=4$–5 mice per group). As described above, the percentage of macrophages in the peritoneal fluid of WT, (**c**) $P2Y_{12}$ knockout and (**d**) $P2Y_{13}$ knockout mice were measured by flow cytometry. PEMs from WT, (**e**) $P2Y_{12}{}^{-/-}$ and (**f**) $P2Y_{13}{}^{-/-}$ mice were treated with ADP (100 μM) for 24 h. Then, the cell supernatants were harvested to measure the concentration of MCP-1 by ELISA. (**g**) BMDM from WT or $P2Y_{12}/P2Y_{13}$ double knockout mice were treated with ADP (100 μM) for 24 h. Then, the cell supernatants were harvested to detect the concentration of MCP-1 by ELISA. (**h**) $P2Y_{13}$ knockout mice were pretreated with prasugrel for 4 h, then these mice and WT mice were injected with either PBS or ADP (50 mg/kg) for 12 h before *E. coli* 0111 injection (1×10^8 CFU). Twelve hours after the injection of *E. coli*, the survival of the mice ($n=6$ in each group) was monitored every 2 h over the next 24 h. The results are presented as the mean ± s.e.m., and each experiment was independently performed three times with 4–5 mice per group as shown. Statistical analysis was performed with Student's *t*-test; $^*P<0.05$, $^{**}P<0.01$, $^{***}P<0.001$. ADP, adenosine 5′-diphosphate; PBS, phosphate-buffered solution; PEM, peritoneal macrophage, i.p., intraperitoneal; WT, wild-type; ELISA, enzyme-linked immunosorbent assay.

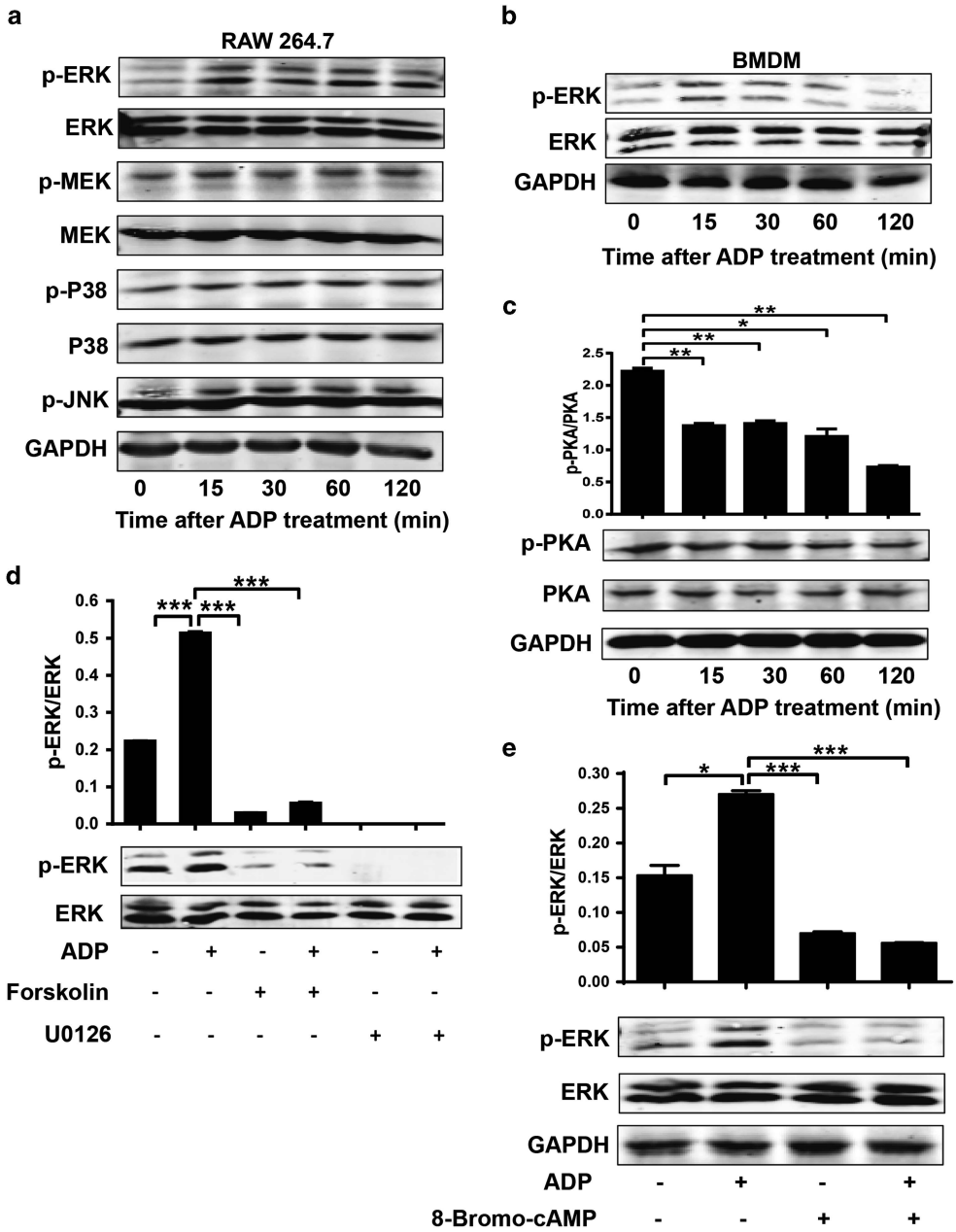

Figure 8 ADP activates cAMP-extracellular signal-regulated kinase (ERK1)2 signaling. (**a**) RAW 264.7 cells and (**b**) BMDMs (only for p-ERK) were stimulated with ADP, and samples from a time course were subjected to western blot analysis to detect the phosphorylation of ERK1/2, JNK and p38 MAPK. (**c**) In addition, the phosphorylation of PKA was measured as described above. RAW 264.7 cells were incubated with or without (**d**) an ERK1/2 inhibitor (U0126, 10 μM), an adenylyl cyclase activator (forskolin, 100 μ) or (**e**) a cAMP-dependent PKA activator (8-Bromo-cAMP, 50 μM) for 30 min before stimulation with 100 μM ADP. Two hours later, the cell lysates were subjected to western blot analysis to detect p-ERK. Semi-quantitative analysis and representative figures are shown. The immunoblot results are representative of at least three independent experiments. The results are expressed as the mean ± s.e.m., and statistical analysis was performed with one-way ANOVA; *$P<0.05$, **$P<0.01$, and ***$P<0.001$ were considered significant differences. ADP, adenosine 5′-diphosphate; cAMP, cyclic AMP; PKA, protein kinase A.

(Figure 9b). Consequently, ADP-induced MCP-1 production could be significantly blocked by forskolin, 8-Bromo-cAMP and U0126 (Figure 9c), suggesting a dominant role of cAMP/PKA/ERK signaling in ADP-mediated immune regulation.

ADP enhances host defense against bacterial infection through cAMP/PKA/ERK signaling

Although it is well known that host defense against invading pathogens can be regulated by different PRRs, the understanding of purinergic signaling in innate immune responses is lacking.

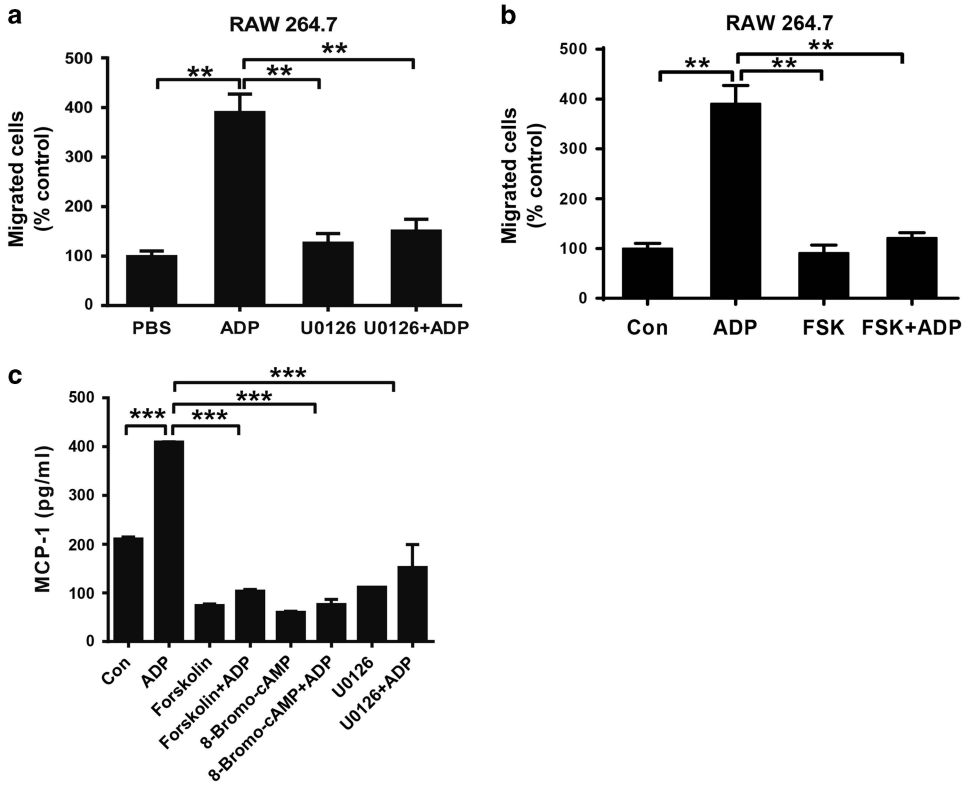

Figure 9 ADP-induced MCP-1 production is dependent on cAMP-ERK1/2. RAW 264.7 cells in 6-well plates were pretreated with (**a**) an ERK1/2 inhibitor (U0126, 10 μM) or (**b**) an adenylyl cyclase activator (forskolin (FSK), 100 μM) for 30 min followed by treatment with 100 μM ADP. Twenty-four hours after the addition of ADP, the supernatants were collected to perform a transwell assay with RAW 264.7 macrophages. The relative counts of migrating cells after treatment were obtained, and representative figures are shown. (**c**) RAW 264.7 cells were pretreated with or without U0126, forskolin or 8-Bromo-cAMP for 30 min before stimulation with ADP for the indicated time, and the MCP-1 levels were measured by ELISA with the cell supernatants. The values are expressed as the mean ± s.e.m., and each experiment was independently performed three times with 4–5 mice per group. Statistical analysis was performed with one-way ANOVA; $^{**}P<0.01$ and $^{***}P<0.001$. ADP, adenosine 5′-diphosphate; ELISA, enzyme-linked immunosorbent assay.

Thus, we pretreated bacterially infected mice with ADP either with or without forskolin. As shown in Figure 10a, the survival of the infected mice was markedly increased by ADP, and this type of protection could be inhibited by forskolin (Figure 10b). Consistent with this, the reduction of bacterial counts by ADP was also blocked by forskolin. In addition, the ADP-mediated recruitment of macrophages (Figure 10c) and MCP-1 production (Figure 10d) was also inhibited by forskolin. It has been shown that the G protein-coupled receptors $P2Y_{12}$ and $P2Y_{13}$ are both $G_{\alpha i}$-coupled receptors that transduce extracellular signals by inhibiting cAMP. Therefore, these data demonstrate that the enhanced innate immune responses by ADP mainly occurs through decreasing the levels of cAMP via the $P2Y_{12}$ or $P2Y_{13}$ receptors (Figure 10e).

DISCUSSION

As a key component involved in the pathophysiology of arterial thrombosis, $P2Y_{12}$ is highly expressed in platelets and has become a major drug target for patients with acute coronary syndrome (ACS).[18] It is well known that platelets have critical roles in inflammation and the immune response. Thus, it is not surprising that increasing clinical evidence has shown that platelet-mediated inflammation could be restricted by clopidogrel, which is a specific inhibitor of $P2Y_{12}$.[19,20] Actually, $P2Y_{12}$ is not only expressed in platelets but is also abundant in macrophages. However, although macrophages are one of most important types of innate immune cells, the role of $P2Y_{12}$ in macrophage-mediated immune responses remains unclear. Here, we demonstrate that the endogenous ligand for $P2Y_{12}$, ADP, is released in both bacterially infected mice and PAMPs-activated macrophages. Furthermore, extracellular ADP protects mice from bacterial infection by increasing MCP-1 to recruit more macrophages to the infected sites. More specifically, ADP-mediated immune regulation occurs mainly through $P2Y_{12}$ and $P2Y_{13}$ but not $P2Y_1$, although $P2Y_1$ is also activated by ADP. In addition, activation of the $P2Y_{12}$ and $P2Y_{13}$ receptors increases ERK signaling and MCP-1 production by inhibiting cAMP. Our study extends the understanding of $P2Y_{12}$ and $P2Y_{13}$ in the regulation of immune responses and provides a theoretical foundation for the clinical application of $P2Y_{12}$/$P2Y_{13}$ in treating ACS and infectious diseases.

The release of endogenous nucleotides initiates the purinergic signaling cascade. Generally, extracellular nucleotides were thought to be mainly nonspecific leakage from dead or injured

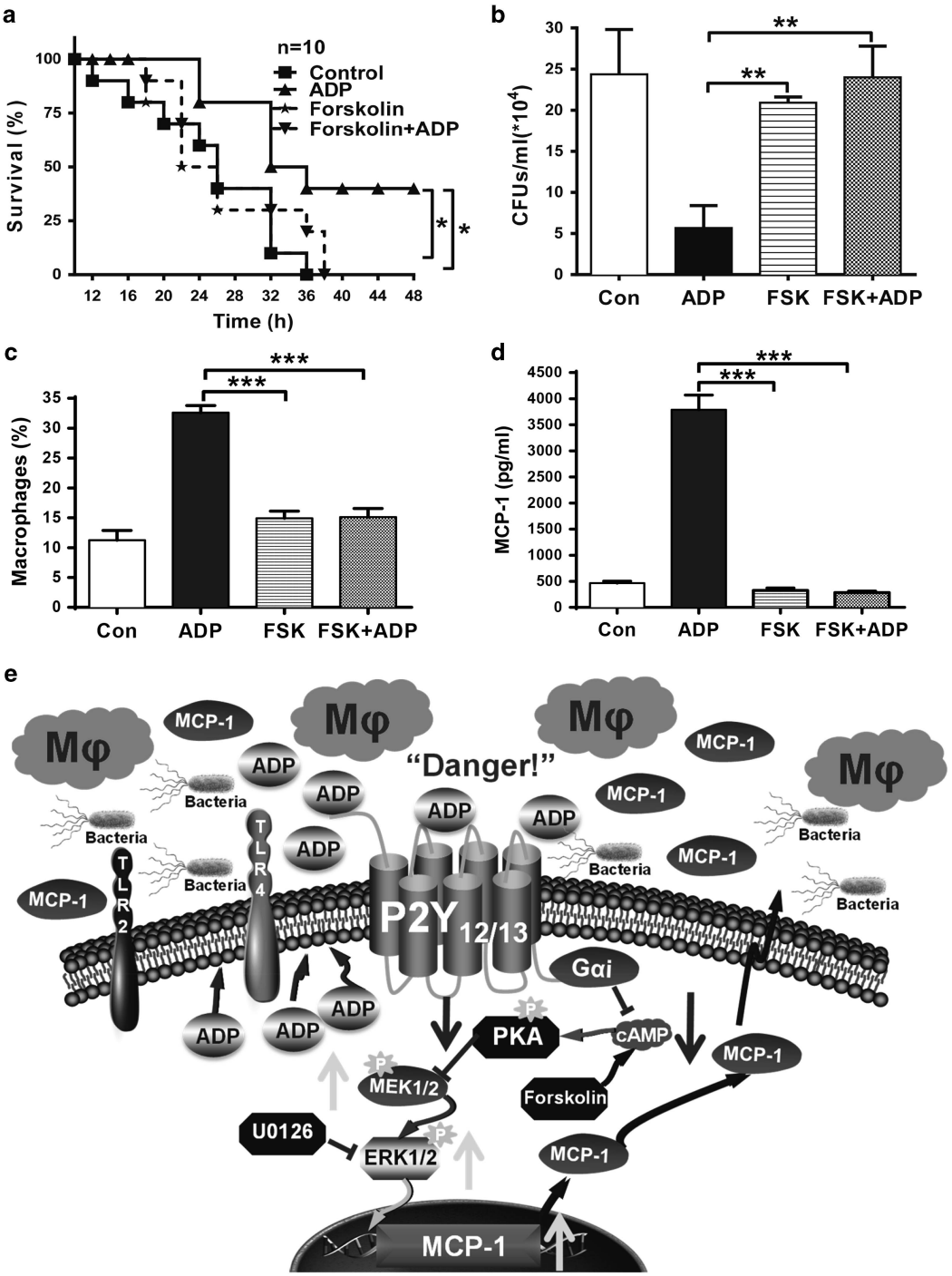

Figure 10 Host defense against invading bacteria was enhanced by ADP/Gαi-coupled P2Y receptors. C57BL/6J mice were pretreated with an injection of PBS, ADP (50 mg/kg), forskolin (100 μM) or forskolin and ADP for 12 h before injection of *E. coli* 0111 (1×10^8 CFU). (**a**) At 12 h after the injection of *E. coli*, the survival of the mice was monitored every 2 h over the following 48 h ($n=10$ mice per group). (**b**) After an additional 12 h, the peritoneal fluid was lavaged from the surviving mice with 3 ml PBS and then diluted 10-fold in PBS, and the bacterial counts were determined by plating on solid LB agar plates ($n=4$–5 mice per group). (**c**) The percentage of macrophages and (**d**) MCP-1 protein levels in the peritoneal fluid of the groups of mice were also measured. (**e**) Proposed model for the role of ADP-induced macrophage recruitment in promoting host defense against invading bacteria through Gαi-coupled P2Y receptor signaling pathways. All values are expressed as the mean ± s.e.m., and each experiment was independently performed three times. Statistical analysis was performed with the log-rank test (**a**) or one-way ANOVA (**b**–**d**); $^{**}P<0.01$ and $^{***}P<0.001$. ADP, adenosine 5′-diphosphate; PBS, phosphate-buffered solution.

cells.[21] However, our previous studies have shown that extracellular nucleotides can be released by immune cells through TLR-activated calcium mobilization or a specific caspase-cleaved pannexin channel.[23] ADP can be secreted from platelet granules or passively released from damaged erythrocytes and endothelial cells, which contributes to the propagation of platelet activation following vascular injury.[24] Interestingly, extracellular ADP is markedly increased after bacterial infection in less than 30 min in both infected mice and PAMPs-treated macrophages in a time- and dose-dependent manner, revealing a relationship between ADP and the innate immune response. Moreover, CD39 and CD73 are extracellular nucleotidase enzymes that catalyze ATP and ADP to adenosine.[25] However, ADP is much more stable than we previously thought; it can be maintained at a high concentration even after 6 h, which provides enough time to facilitate an innate immune response. Thus, these data support a role for extracellular ADP in fighting against invading pathogens. In addition, adenosine from degraded ADP may be involved in inflammatory resolution and exert a negative regulation after excessively activated inflammatory responses by preventing the differentiation of monocytes and inhibiting the production of inflammatory mediators.[26,27]

Circulating monocytes derived from precursors in the bone marrow[28] mediate the host antimicrobial defense[29] as well as many inflammatory diseases, such as atherosclerosis.[30] On the basis of chemokine receptors and surface molecule expression, monocytes can be divided into different subtypes that have remarkable multipotency. Among the multiple subtypes, monocytes with high levels of CC-chemokine receptor 2 (CCR2) and Ly6C are often referred to as inflammatory monocytes, which are rapidly recruited to sites of infection and inflammation. CCR2 deficiency decreases the host defense against invading pathogens through reduced monocyte recruitment.[31,32] However, monocytes with low levels of CCR2 mainly adhere to and migrate along the luminal surface of endothelial cells that line the small blood vessels to patrol[33] and facilitate tissue repair.[34] Therefore, the secretion of CCL-2 (MCP-1) is crucial in recruiting $CCR2^{high}$ monocytes for antibacterial immune responses. We demonstrated a significant increase in CCL-2 levels in ADP-treated cells and mice, which could be the main mechanism underlying ADP-mediated protection against bacterial infection. Accordingly, a significant increase in CD11b- and F4/80-positive cells were found in ADP-treated mice. Furthermore, ADP-treated cell supernatants also enhanced the migration of macrophages. For this reason, ADP-mediated protection could mainly occur through the recruitment of more $CCR2^{high}$ monocytes to clear the invading bacteria.

The canonical second messenger cAMP, which is produced from ATP by adenylyl cyclase (AC), is well-established as a potent negative regulator of T cell immune function through PKA signaling.[35] At the same time, the activity of AC can be regulated by GPCRs through their $G_{\alpha i}$ and $G_{\alpha s}$ subunits.[36] Interestingly, $P2Y_{12}$ and $P2Y_{13}$ belong to the $P2Y_{12}$-like subfamily of proteins, which bind with $G_{\alpha i}$ to inhibit AC and reduce the cAMP intracellular levels.[37] However, in this study, we found that $P2Y_1$, which can activate Ca^{2+}-associated signaling through the $G_{\alpha q}$ subunit, is dispensable for ADP-mediated immune regulation. In single $P2Y_{12}$ and $P2Y_{13}$ knockout mice, the ADP-mediated immune regulation could be partially rescued, but we do not have double knockout mice to fully block ADP-activated $G_{\alpha i}$ signaling. In cells from single knockout mice, if we pretreated with forskolin (a direct activator of AC), the ADP-mediated immune response was totally blocked, suggesting the dominant role of cAMP in this process. Furthermore, we also found that the expression of $P2Y_{13}$ was markedly increased in both PAMP-activated cells and tuberculosis patients. Taken together, the release of endogenous ADP and the significantly enhanced expression of $P2Y_{13}$ reveal the great potential of ADP-associated signaling in fighting against infectious diseases, which extends our understanding of the clinical application of $P2Y_{12}$/$P2Y_{13}$-based antiplatelet drugs. This study revealed that ADP can be regarded as an immunomodulatory molecule in regulating innate immunity against bacterial infection, which suggests the potential therapeutic significance of the ADP/P2Y-associated signaling in preventing and controlling bacterial diseases and lays a theoretical foundation for immunoregulation-based antibacterial therapies.

CONFLICT OF INTEREST

The authors declare no conflict of interest.

ACKNOWLEDGEMENTS

This work was supported by the National Basic Research Program of China (2012CB910400), the National Natural Science Foundation of China (81272369, 31470040, 31570896 and 81672811), the Doctoral Fund of Ministry of Education of China (20130076110013); Science and Technology Commission of Shanghai Municipality (15JC1401500).

1 Janeway CA, Medzhitov R. Innate immune recognition. *Ann Rev Immunol* 2002; **20**: 197–216.
2 Medzhitov R. Recognition of microorganisms and activation of the immune response. *Nature* 2007; **449**: 819–826.
3 Pedra JHF, Cassel SL, Sutterwala FS. Sensing pathogens and danger signals by the inflammasome. *Curr Opin Immunol* 2009; **21**: 10–16.
4 Paoletti A, Raza SQ, Voisin L, Law F, Pipoli da Fonseca J, Caillet M *et al.* Multifaceted roles of purinergic receptors in viral infection. *Microbes Infect* 2012; **14**: 1278–1283.
5 Tang D, Kang R, Coyne CB, Zeh HJ, Lotze MT. PAMPs and DAMPs: signal Os that spur autophagy and immunity. *Immunol Rev* 2012; **249**: 158–175.
6 Ralevic V, Burnstock G. Receptors for purines and pyrimidines. *Pharmacol Rev* 1998; **50**: 413–492.
7 Chen Y, Corriden R, Inoue Y, Yip L, Hashiguchi N, Zinkernagel A *et al.* ATP release guides neutrophil chemotaxis via P2Y2 and A3 receptors. *Science* 2006; **314**: 1792–1795.
8 Bednash JS, Mallampalli RK. Regulation of inflammasomes by ubiquitination. *Cell Mol Immunol* 2016.
9 Jo EK, Kim JK, Shin DM, Sasakawa C. Molecular mechanisms regulating NLRP3 inflammasome activation. *Cell Mol Immunol* 2016; **13**: 148–159.
10 Ren H, Teng Y, Tan B, Zhang X, Jiang W, Liu M *et al.* Toll-like receptor-triggered calcium mobilization protects mice against bacterial infection

through extracellular ATP release. *Infect Immun* 2014; **82**: 5076–5085.
11 Gendron FP, Benrezzak O, Krugh BW, Kong Q, Weisman GA, Beaudoin AR. Purine signaling and potential new therapeutic approach: possible outcomes of NTPDase inhibition. *Curr Drug Targets* 2002; **3**: 229–245.
12 Yegutkin GG. Nucleotide- and nucleoside-converting ectoenzymes: Important modulators of purinergic signalling cascade. *Biochim Biophys Acta* 2008; **1783**: 673–694.
13 Paruchuri S, Tashimo H, Feng C, Maekawa A, Xing W, Jiang Y *et al.* Leukotriene E4-induced pulmonary inflammation is mediated by the P2Y12 receptor. *J Exp Med* 2009; **206**: 2543–2555.
14 Woodford N, Turton JF, Livermore DM. Multiresistant Gram-negative bacteria: the role of high-risk clones in the dissemination of antibiotic resistance. *FEMS Microbiol Rev* 2011; **35**: 736–755.
15 Hawkey PM, Jones AM. The changing epidemiology of resistance. *J Antimicrob Chemother* 2009; **64**: i3–i10.
16 Cai Y, Yang Q, Tang Y, Zhang M, Liu H, Zhang G *et al.* Increased complement C1q level marks active disease in human tuberculosis. *PLoS One* 2014; **9**: e92340.
17 Qin J, Zhang G, Zhang X, Tan B, Lv Z, Liu M *et al.* TLR-activated gap junction channels protect mice against bacterial infection through extracellular UDP release. *J Immunol* 2016; **196**: 1790–1798.
18 Topol EJ, Schork NJ. Catapulting clopidogrel pharmacogenomics forward. *Nat Med* 2011; **17**: 40–41.
19 Chen YG, Xu F, Zhang Y, Ji QS, Sun Y, Lu RJ *et al.* Effect of aspirin plus clopidogrel on inflammatory markers in patients with non-ST-segment elevation acute coronary syndrome. *Chin Med J* 2006; **119**: 32–36.
20 Gurbel PA, Bliden KP, Tantry US. Effect of clopidogrel with and without eptifibatide on tumor necrosis factor-alpha and C-reactive protein release after elective stenting: results from the clear platelets 1b study. *J Am Coll Cardiol* 2006; **48**: 2186–2191.
21 Bours MJ, Swennen EL, Di Virgilio F, Cronstein BN, Dagnelie PC. Adenosine 5'-triphosphate and adenosine as endogenous signaling molecules in immunity and inflammation. *Pharmacol Ther* 2006; **112**: 358–404.
22 Li R, Tan B, Yan Y, Ma X, Zhang N, Zhang Z *et al.* Extracellular UDP and P2Y6 function as a danger signal to protect mice from vesicular stomatitis virus infection through an increase in IFN-beta production. *J Immunol* 2014; **193**: 4515–4526.
23 Woulfe D, Yang J, Brass L. ADP and platelets: the end of the beginning. *J Clin Invest* 2001; **107**: 1503–1505.
24 Hasko G, Linden J, Cronstein B, Pacher P. Adenosine receptors: therapeutic aspects for inflammatory and immune diseases. *Nat Rev Drug Discov* 2008; **7**: 759–770.
25 Najar HM, Ruhl S, Bru-Capdeville AC, Peters JH. Adenosine and its derivatives control human monocyte differentiation into highly accessory cells versus macrophages. *J Leukoc Biol* 1990; **47**: 429–439.
26 Haskó G, Kuhel DG, Chen J-F, Schwarzschild MA, Deitch EA, Mabley JG *et al.* Adenosine inhibits IL-12 and TNF-α production via adenosine A2a receptor-dependent and independent mechanisms. *FASEB J* 2000; **14**: 2065–2074.
27 van Furth R, Cohn ZA. The origin and kinetics of mononuclear phagocytes. *J Exp Med* 1968; **128**: 415–435.
28 Serbina NV, Jia T, Hohl TM, Pamer EG. Monocyte-mediated defense against microbial pathogens. *Annu Rev Immunol* 2008; **26**: 421–452.
29 Woollard KJ, Geissmann F. Monocytes in atherosclerosis: subsets and functions. *Nat Rev Cardiol* 2010; **7**: 77–86.
30 Kurihara T, Warr G, Loy J, Bravo R. Defects in macrophage recruitment and host defense in mice lacking the CCR2 chemokine receptor. *J Exp Med* 1997; **186**: 1757–1762.
31 Kuziel WA, Morgan SJ, Dawson TC, Griffin S, Smithies O, Ley K *et al.* Severe reduction in leukocyte adhesion and monocyte extravasation in mice deficient in CC chemokine receptor 2. *Proc Natl Acad Sci USA* 1997; **94**: 12053–12058.
32 Auffray C, Fogg D, Garfa M, Elain G, Join-Lambert O, Kayal S *et al.* Monitoring of blood vessels and tissues by a population of monocytes with patrolling behavior. *Science* 2007; **317**: 666–670.
33 Nahrendorf M, Swirski FK, Aikawa E, Stangenberg L, Wurdinger T, Figueiredo JL *et al.* The healing myocardium sequentially mobilizes two monocyte subsets with divergent and complementary functions. *J Exp Med* 2007; **204**: 3037–3047.
34 Mosenden R, Tasken K. Cyclic AMP-mediated immune regulation—overview of mechanisms of action in T cells. *Cell Signal* 2011; **23**: 1009–1016.
35 Zhu N, Cui J, Qiao C, Li Y, Ma Y, Zhang J *et al.* cAMP modulates macrophage development by suppressing M-CSF-induced MAPKs activation. *Cell Mol Immunol* 2008; **5**: 153–157.
36 Vitiello L, Gorini S, Rosano G, la Sala A. Immunoregulation through extracellular nucleotides. *Blood* 2012; **120**: 511–518.